

## Pure spin currents induced by spin-dependent scattering processes in SiGe quantum well structures

S. D. Ganichev,<sup>1</sup> S. N. Danilov,<sup>1</sup> V. V. Bel'kov,<sup>1,2</sup> S. Giglberger,<sup>1</sup> S. A. Tarasenko,<sup>2</sup> E. L. Ivchenko,<sup>2</sup> D. Weiss,<sup>1</sup> W. Jantsch,<sup>3</sup> F. Schäffler,<sup>3</sup> D. Gruber,<sup>3</sup> and W. Prettl<sup>1</sup>

<sup>1</sup>*Fakultät Physik, Universität Regensburg, 93040 Regensburg, Germany*

<sup>2</sup>*A.F. Ioffe Physico-Technical Institute, Russian Academy of Sciences, 194021 St. Petersburg, Russia*

<sup>3</sup>*Institut für Halbleiter und Festkörperphysik, Johannes-Kepler Universität Linz, A-4040 Linz, Austria*

(Received 30 October 2006; revised manuscript received 21 December 2006; published 13 April 2007)

We show that spin-dependent electron-phonon interaction in the energy relaxation of a two-dimensional electron gas results in equal and oppositely directed currents in the spin-up and spin-down subbands yielding a pure spin current. In our experiments on SiGe heterostructures the pure spin current is converted into an electric current applying a magnetic field that lifts the cancellation of the two partial charge flows. A microscopic theory of this effect, taking account of the asymmetry of the relaxation process, is developed and is in good agreement with the experimental data.

DOI: [10.1103/PhysRevB.75.155317](https://doi.org/10.1103/PhysRevB.75.155317)

PACS number(s): 73.21.Fg, 72.25.Fe, 78.67.De, 73.63.Hs

Lately, there has been much interest in the use of the spin of carriers in semiconductor quantum well (QW) structures together with their charge to realize concepts such as spintronics and spin-optoelectronics.<sup>1</sup> The transport of the spin of charge carriers in semiconductor nanostructures is one of the key problems in this field. Among the necessary conditions to realize spintronics devices there are a high spin polarization in QWs and a large spin splitting of subbands. The latter is important to control spins by an external electric field via the Rashba effect.<sup>2</sup> While most of the investigations aimed at spintronics and spin-optoelectronics have been carried out on III-V compounds, some recent results obtained on nonmagnetic SiGe nanostructures applying electron spin resonance<sup>3,4</sup> (ESR) and the circular photogalvanic effect (CPGE),<sup>5,6</sup> demonstrated that this material may be a promising system for spin-based electronics. ESR and CPGE data show that spin relaxation times in SiGe QWs can be sufficiently long,<sup>3,4,7–11</sup> that the spin degeneracy is lifted,<sup>3,5,6,11,12</sup> that the  $g$  factor is tunable by crystallographic direction, electron density, Ge content, kinetic energy of free carriers, and electric current<sup>3,13–17</sup> and that spin manipulation can be achieved by means of the spin-echo method.<sup>4</sup>

Here we report on an electrically measured observation of pure spin currents causing spatial spin separation in SiGe quantum well structures, allowing manipulation of spins in this material which is attractive for high-speed electronics and spintronics. Spin currents recently attracted rapidly growing interest since they can provide new tools for the realization of all-electric nonmagnetic semiconductor spintronics. Various phenomena comprising charge photocurrents driven by the spin degree of freedom<sup>18–26</sup> and spin separation caused by pure spin currents<sup>27–32</sup> were reported. Most of these phenomena originate from the well known lifting of spin degeneracy. The latter causes the band structure to split into spin-up and spin-down branches described by linear in wave vector  $\mathbf{k}$  terms in the Hamiltonian due to structure inversion asymmetry (SIA) or bulk inversion asymmetry (BIA). The pure spin currents reported here are caused by less known spin-dependent electron scattering processes<sup>33,34</sup> which generate a pure spin current, causing spin separation

in a similar way as in the spin Hall effect.<sup>30,31,35–37</sup> In contrast to the latter, no external bias needs to be applied.<sup>32</sup>

Spin separation due to spin-dependent scattering in gyrotropic media can be achieved in various ways but all of them must drive the electron gas into a nonequilibrium state. One straightforward method used here is to heat the electron system by terahertz (THz) or microwave radiation.

Figure 1(a) sketches the process of energy relaxation of hot electrons for the spin-up subband ( $s = +1/2$ ) in a quantum well containing a two-dimensional electron gas (2DEG). Energy relaxation processes are shown by curved arrows. Usually, energy relaxation via scattering of electrons is considered to be spin-independent. In gyrotropic media, such as low-dimensional GaAs structures or asymmetric SiGe QWs investigated here, however, spin-orbit interaction adds an asymmetric spin-dependent term to the scattering probability.<sup>32</sup> This term in the scattering matrix element is proportional to components of  $[\boldsymbol{\sigma} \times (\mathbf{k} + \mathbf{k}')]_x$ , where  $\boldsymbol{\sigma}$  is the vector composed of the Pauli matrices,  $\mathbf{k}$  and  $\mathbf{k}'$  are the initial and scattered electron wave vectors.<sup>38</sup> Due to spin-dependent scattering, transitions to positive and negative  $k'_x$  states occur with different probabilities. Therefore hot electrons with opposite  $k_x$  have different relaxation rates in the two spin subbands. In Fig. 1(a) this difference is indicated by arrows of different thickness. This asymmetry causes an imbalance in the distribution of carriers in both subbands ( $s = \pm 1/2$ ) between positive and negative  $k_x$  states. This in turn yields a net electron flow  $i_{\pm 1/2}$  within each spin subband. Since the asymmetric part of the scattering amplitude depends on spin orientation, the probabilities for scattering to positive or negative  $k'_x$  states are inverted for spin-down and spin-up subbands. Thus, the charge currents  $j_+ = ei_{+1/2}$  and  $j_- = ei_{-1/2}$ , where  $e$  is the electron charge, have opposite directions because  $i_{+1/2} = -i_{-1/2}$  and therefore they cancel each other. Nevertheless, a finite pure spin current  $J_{\text{spin}} = \frac{1}{2}(i_{+1/2} - i_{-1/2})$  is generated since electrons with spin-up and spin-down move in opposite directions.<sup>32</sup> This leads to a spatial spin separation and spin accumulation at the edges of the sample. In the above analysis we do not consider the effect of a  $\mathbf{k}$ -linear spin splitting of the electron subband since it

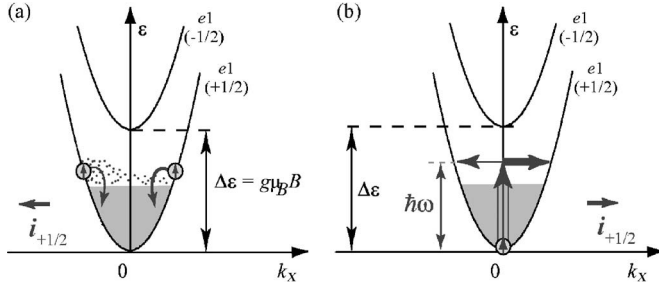


FIG. 1. Microscopic origin of a zero-bias spin separation and the corresponding magnetic field-induced photocurrent. Zero-bias spin separation is due to scattering matrix elements linear in  $\mathbf{k}$  and  $\boldsymbol{\sigma}$  causing asymmetric scattering and it results in spin flows. This process is sketched for the spin-up subband only and for (a) energy relaxation and (b) excitation via indirect transitions (Drude-like absorption). Here, scattering is assumed to have a larger probability for positive  $k_x$  than that for negative  $k_x$  as indicated by arrows of different thickness. Therefore in (a) the energy relaxation rates for positive  $k_x$  are larger than for negative  $k_x$  and in (b) the rates of optical transitions for opposite wave vectors are different. This imbalance leads to a net spin-up electron flow. In the spin-down subband the picture is mirror symmetric, resulting in a net spin-down electron flow of opposite direction. Thus at zero magnetic field a pure spin current is generated. The corresponding electric currents have equal magnitudes and therefore cancel each other. An in-plane magnetic field, however, lifts the compensation of the oppositely directed electron flows yielding a charge current.

does not lead to a significant contribution to the pure spin current. In fact, to first order in spin-orbit interaction, the spin splitting of the subband results only in a relative displacement of the spin-up and spin-down branches in  $\mathbf{k}$  space. This shift does not disturb the symmetric distribution of carriers within each subband even if the system is driven into a nonequilibrium state, e.g., by absorption of linearly polarized radiation. Hence spin-splitting in  $\mathbf{k}$  space has no essential effect on the mechanism of spin-separation discussed here and can affect it only in high-order approximations.

Similar to the relaxation mechanism, optical excitation of free carriers by Drude absorption, also involving electron scattering, is asymmetric and yields spin separation.<sup>32</sup> Drude absorption is caused by indirect intraband optical transitions and includes a momentum transfer from phonons or impurities to electrons to satisfy momentum conservation. Figure 1(b) sketches the process of Drude absorption via virtual states for the spin-up subband. Vertical arrow indicates optical transitions from the initial state with electron wave vector  $k_x=0$  while the horizontal arrows describe an elastic scattering event to a final state with either positive or negative electron wave vector. Due to the spin dependence of scattering, transitions to positive and negative  $k_x$  states occur with different probabilities. This is indicated by the different thickness of the horizontal arrows. The asymmetry causes an imbalance in the distribution of photoexcited carriers in the spin subband between positive and negative  $k_x$  states. This in turn yields electron flow. As for the relaxation mechanism described above probabilities for scattering to positive or negative  $k_x$  are inverted for spin-down and spin-up subbands and spin separation takes place. We described this mecha-

nism in detail in previous publications.<sup>29,32</sup> The model and the theoretical considerations described there can be directly applied to SiGe structures. Spin separation due to hot electron energy relaxation, in contrast, was only briefly addressed in Ref. 32 and is therefore discussed in greater details here.

A pure spin current and zero-bias spin separation can be converted into a measurable electric current by application of a magnetic field.<sup>32</sup> Indeed, in a Zeeman spin-polarized system, the two fluxes  $i_{\pm 1/2}$ , whose magnitudes depend on the free carrier densities in spin-up and spin-down subbands,  $n_{\pm 1/2}$ , respectively, do no longer compensate each other and hence yield a net electric current (see Fig. 1). For the case, where the fluxes  $i_{\pm 1/2}$  are proportional to the carrier densities  $n_{\pm 1/2}$ ,<sup>39</sup> the charge current is given by

$$\mathbf{j} = e(i_{+1/2} + i_{-1/2}) = 4eS\mathbf{J}_{\text{spin}}, \quad (1)$$

where  $S = \frac{1}{2}(n_{+1/2} - n_{-1/2}) / (n_{+1/2} + n_{-1/2})$  is the magnitude of the average spin. An external magnetic field  $\mathbf{B}$  results in different populations of the two spin subbands due to the Zeeman effect. In equilibrium the average spin is given by

$$S = -\frac{g\mu_B \mathbf{B}}{4\bar{\epsilon}}. \quad (2)$$

Here  $g$  is the electron effective  $g$  factor,  $\mu_B$  the Bohr magneton,  $\bar{\epsilon}$  the characteristic electron energy being equal to the Fermi energy  $\epsilon_F$ , or to the thermal energy  $k_B T$ , for a degenerate or a nondegenerate 2DEG, respectively.<sup>40</sup>

To demonstrate the existence of the spin-polarized current described above we chose the following experimental conditions: electron gas heating is achieved by absorption of linearly polarized THz radiation at normal incidence on a (001)-grown QW. Spin polarization is obtained by an in-plane magnetic field and the current is measured both in the directions normal and parallel to the magnetic field.

The chosen experimental geometry excludes other effects that are known to cause photocurrents in (001)-oriented QWs: since linearly polarized radiation is used, all helicity-dependent spin photocurrents, such as the circular photogalvanic effect<sup>18</sup> and the spin-galvanic effect,<sup>19</sup> are absent. In addition, photon drag and the linear photogalvanic effect are forbidden by symmetry for normal incidence on (001)-grown heterostructure (see, e.g., Refs. 20, 22, and 24).

The measurements are carried out on  $n$ -type SiGe QW structures, MBE-grown on (001)-oriented Si substrates. The samples contain a single, 15 nm wide, strained Si quantum well deposited on a 3  $\mu\text{m}$  thick graded buffer ramping to a composition of  $\text{Si}_{0.75}\text{Ge}_{0.25}$ . On top of the tensilely strained Si quantum well a second  $\text{Si}_{0.75}\text{Ge}_{0.25}$  barrier is grown containing  $10^{18} \text{ cm}^{-3}$  of Sb for modulation doping. Due to the one-sided doping, the two-dimensional electron gas channel has structure inversion asymmetry. Two samples with free carrier densities of  $2.8 \times 10^{11} \text{ cm}^{-2}$  (sample 1) and  $3.5 \times 10^{11} \text{ cm}^{-2}$  (sample 2) and corresponding low temperature mobilities (1.5 K) of  $1.7 \times 10^5 \text{ cm}^2/\text{V s}$  and  $1.0 \times 10^5 \text{ cm}^2/\text{V s}$ , respectively, are studied. Two pairs of

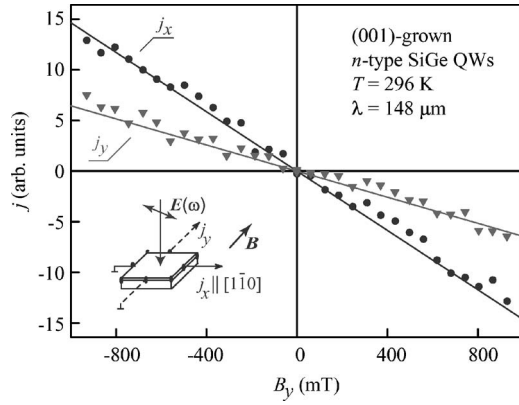


FIG. 2. Magnetic field dependence of the photocurrent  $j$  measured in sample 1 at room temperature with the magnetic field  $\mathbf{B}$  parallel to the  $y$  direction. Radiation of power  $P \approx 15$  kW is applied at normal incidence. Circles show results obtained for  $\mathbf{j} \perp \mathbf{B}$ , obtained for the radiation polarized perpendicularly to the magnetic field ( $\alpha=0^\circ$ ). Triangles show current  $\mathbf{j} \parallel \mathbf{B}$ . These data are given for  $\alpha=135^\circ$ , inset shows the experimental geometry.

Ohmic contacts in the center of the sample edges oriented along  $x \parallel [1\bar{1}0]$  and  $y \parallel [110]$  have been prepared (see inset in Fig. 2).

A high power THz molecular laser, optically pumped by a TEA-CO<sub>2</sub> laser,<sup>24</sup> has been used to deliver 100 ns pulses of linearly polarized radiation with a power of about 15 kW at a wavelength of  $\lambda = 148 \mu\text{m}$ . The radiation causes indirect optical transitions within the lowest size-quantized subband. The samples are irradiated along the growth direction. An external magnetic field  $B$  up to 1 T is applied parallel to the interface plane. The current  $\mathbf{j}$ , generated by the light in the unbiased devices, is measured via the voltage drop across a 50  $\Omega$  load resistor in a closed-circuit configuration. The voltage is recorded with a storage oscilloscope. Measurements are carried out in a wide temperature range from liquid helium to room temperature. The measured current pulses follow the temporal structure of the applied laser pulses. In experiment the angle  $\alpha$  between the polarization plane of the light and  $x$  axis is varied. This is achieved by a  $\lambda/2$  plate which enables us to vary the angle  $\alpha$  between  $0^\circ$  and  $180^\circ$ .

Irradiation of the samples at zero magnetic field does not lead to any signal as expected from the microscopic mechanism described above as well as from the phenomenological analysis. A current response, however, is obtained when a magnetic field is applied. Figure 2 shows the magnetic field dependence of the photocurrent for two directions: along and perpendicular to the in-plane magnetic field  $\mathbf{B}$  (the latter is aligned along  $y$ ). The current increases linearly with  $\mathbf{B}$  and changes sign upon the reversal of the magnetic field direction. This is in agreement with the above model because the strength and direction of the magnetic field affects the average spin and therefore the electric current, as given in Eqs. (1) and (2).

Figures 3 and 4 show the dependencies of the current on polarization and temperature, respectively. We found that the polarization dependence of the current can be fitted by  $j_x = j_1 \cos 2\alpha + j_2$  for the transverse geometry and by  $j_y = j_3 \sin 2\alpha$  for the longitudinal geometry in the whole

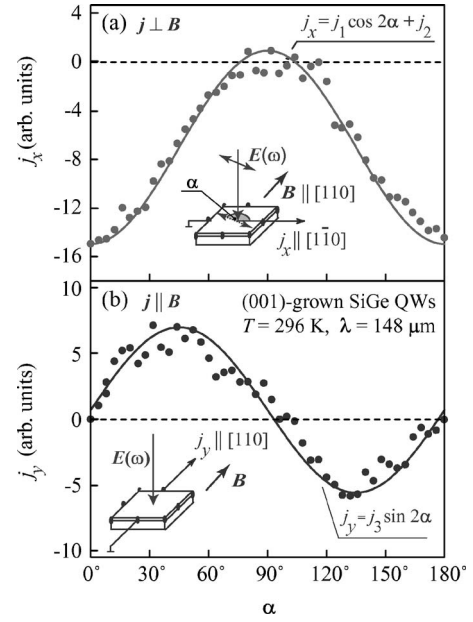


FIG. 3. Photocurrent in sample 1 as a function of  $\alpha$ . The sample is excited by normally incident linearly polarized radiation of power  $P \approx 17$  kW. Data are obtained at room temperature for a magnetic field of  $B_y = 1$  T. (a) Photocurrent for  $\mathbf{j} \perp \mathbf{B} \parallel y$ . Line: fit of  $j_x = j_1 \cos 2\alpha + j_2$ . (b) Photocurrent for  $\mathbf{j} \parallel \mathbf{B} \parallel y$ . Line is fitted to  $j_y = j_3 \sin 2\alpha$ . The insets show the experimental geometries.

range of temperature. These polarization dependencies are in accordance with the phenomenological theory of magnetic field induced photocurrents.<sup>41</sup> As shown in Ref. 32, the currents  $j_1$  and  $j_3$  are caused by indirect optical transitions and therefore exhibit polarization dependence. In contrast, the current  $j_2$  is driven by energy relaxation of hot electrons and is therefore independent of the light polarization. It is expected and observed only for transverse geometry.<sup>41</sup> Using two fixed polarization directions in the transverse geometry  $\alpha=0^\circ$  and  $\alpha=90^\circ$  allows us to extract both contributions. Adding and subtracting the currents of both orientations the coefficients  $j_1$  (polarization-dependent amplitude) and  $j_2$  (polarization-independent background) can be obtained by

$$j_1 = \frac{j_x(0^\circ) - j_x(90^\circ)}{2}, \quad j_2 = \frac{j_x(0^\circ) + j_x(90^\circ)}{2}. \quad (3)$$

Figure 4 shows the temperature dependencies of  $j_1$ ,  $j_2$  and the electron density  $n_s$ . Below 100 K both current contributions are almost independent of temperature, but at temperatures above 150 K the current strength decreases with increasing temperature.

The peculiar temperature and polarization dependencies are a clear-cut proof that the observed charge current is a result of imbalanced spin currents. Let us first consider the temperature behavior of the polarization-dependent  $j_1$  contribution caused by asymmetric excitation. As has been shown in Ref. 32, for fixed polarization and certain scattering mechanism, e.g., phonon or impurity scattering, the temperature dependence of magneto-photocurrent due to this mechanism is described by  $j_1/I \propto \tau_p \eta(\omega)S$ . Here  $I$  is the radiation intensity,<sup>39</sup>  $\tau_p$  is the momentum relaxation time,  $\eta(\omega)$  is the



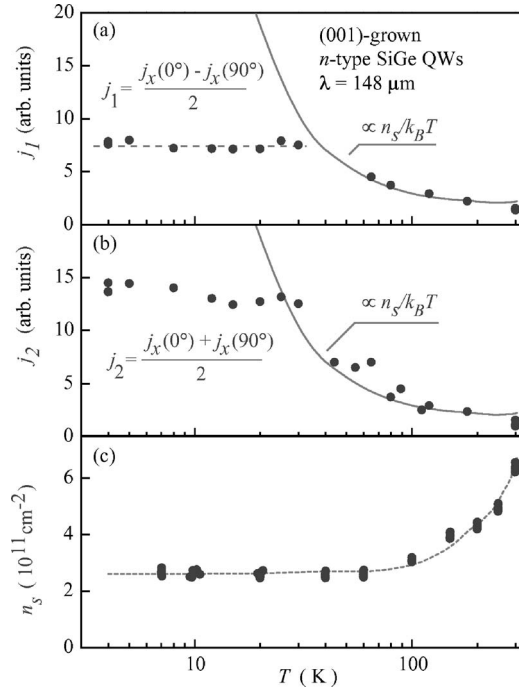


FIG. 4. (a) and (b) Temperature dependencies of the transverse photocurrent. Data are obtained for  $B_y = -0.6$  T applied to sample 1 and an excitation power of  $P \approx 5$  kW. Photocurrents  $j_1(T)$  (a) and  $j_2(T)$  (b), obtained by subtracting and adding the currents for the two polarizations  $\alpha = 0^\circ$  and  $\alpha = 90^\circ$ . (c) Temperature dependence of the carrier density  $n_s$ . Full lines are fits to  $An_s/k_B T$  with a single fitting parameter  $A$ . The dotted line is meant as a guide for eye.

QW absorbance, and  $\omega$  is the radiation frequency. Since for Drude absorption and  $\omega\tau_p \gg 1$  the absorbance is given by  $\eta(\omega) \propto n_s/\tau_p$  (see Ref. 42), the momentum relaxation time  $\tau_p$  cancels and the temperature dependence of the current reduces to  $j_1 \propto n_s S$ . At low temperatures  $S \propto 1/\varepsilon_F \propto 1/n_s$  [see Eq. (2)] and the current  $j_1 \propto n_s S$  becomes independent of temperature as observed in our experiment [see dashed line in Fig. 4(a)]. In additional experiments we change the carrier density at 4.2 K by visible and near infrared light. By that the carrier density (mobility) increases from  $2.8 \times 10^{11} \text{ cm}^{-2}$  ( $1.7 \times 10^5 \text{ cm}^2/\text{V s}$ ) to  $3.6 \times 10^{11} \text{ cm}^{-2}$  ( $2.2 \times 10^5 \text{ cm}^2/\text{V s}$ ) for sample 1 after illumination at low  $T$ . Though both  $n_s$  and  $\tau_p$  increase by about 30%, the photocurrent remains unchanged, thus confirming the above arguments. For high temperatures the carrier distribution is sufficiently well described by the Boltzmann function and hence  $S \propto 1/k_B T$  [see Eq. (2)]. Therefore, the current is proportional to  $n_s/k_B T$  and decreases with increasing temperature in agreement to experiment [see solid line in Fig. 4(a), showing the fit of data to  $n_s/T$ , obtained with one ordinate scaling parameter]. In the intermediate range between 25 and 100 K, such simple analysis fails. In this temperature range the scattering mechanism changes from impurity dominated to phonon dominated. This region is not yet considered theoretically.

The theoretical treatment of the photocurrent contribution due to the excitation mechanisms [Fig. 1(b)] was developed in Ref. 32 and describes the dependencies of  $j_1$  and  $j_3$  on

magnetic field, polarization, and temperature quite well. To describe the polarization independent contribution  $j_2$  we develop the microscopic theory of the magnetoinduced photocurrent caused by energy relaxation. Our treatment is based on the spin-density-matrix formalism and presented here for acoustic phonon mediated electron scattering. The energy relaxation of spin-polarized hot carriers in gyrotropic structures and in the presence of a magnetic field is accompanied by the generation of an electric current which is given by

$$j_{\text{rel}} = 2e \sum_{kk'} \sum_{s=\pm 1/2} (\mathbf{v}_k - \mathbf{v}_{k'}) \tau_p f_{k's} (1 - f_{ks}) w_{ks \leftarrow k's}, \quad (4)$$

where the index  $s$  designates the spin state,  $\mathbf{v}_k = \hbar \mathbf{k}/m^*$  is the velocity,  $m^*$  the effective electron mass,  $f_{ks}$  the distribution function of carriers in the spin subband  $s$ ,  $w_{ks \leftarrow k's}$  the rate of phonon-induced electron scattering, and the factor 2 in Eq. (4) accounts for the valley degeneracy in SiGe (001)-grown QW structures. The scattering rate has the form

$$w_{ks \leftarrow k's} = \frac{2\pi}{\hbar} \sum_{q,\pm} |M_{ks,k's}|^2 \left( N_q + \frac{1}{2} \pm \frac{1}{2} \right) \delta(\varepsilon_k - \varepsilon_{k'} \pm \hbar \Omega_q), \quad (5)$$

where  $\Omega_q$  and  $\mathbf{q}$  are the frequency and wave vector of the phonon involved,  $M_{ks,k's}$  is the matrix element of electron-phonon interaction,  $N_q$  the phonon occupation number,  $\varepsilon_k = \hbar^2 \mathbf{k}^2/2m^*$  the electron kinetic energy, and the signs “ $\pm$ ” correspond to the phonon emission and absorption. We note that, as discussed above,  $\mathbf{k}$ -linear spin splitting of the energy spectrum is not important for the mechanism under study.

For the structure symmetry described by the axial  $C_{\infty v}$  point group, which is obviously relevant for the SiGe-based QWs under study, the matrix element of electron-phonon interaction can be modeled by

$$M_{k,k'} = A(q_z) + B(q_z) [\sigma_x(k_y + k'_y) - \sigma_y(k_x + k'_x)], \quad (6)$$

where  $A(q_z)$  and  $B(q_z)$  are material parameters determined by the QW structure and  $q_z$  is the phonon wave vector component along the growth direction. Further we assume that the inequality  $q_x, q_y \ll q_z$  is fulfilled for the typical phonons involved.

We consider heating of the electron gas by radiation and that the electron temperature (the same for both spin subbands) slightly exceeds the lattice temperature. Then, using the Boltzmann distribution of the carriers for the nondegenerate case (the high-temperature range) and in the quasielastic approximation, one derives

$$j_{\text{rel},x} = 4e\tau_p S_y \xi I \eta / \hbar, \quad j_{\text{rel},y} = -4e\tau_p S_x \xi I \eta / \hbar, \quad (7)$$

where  $\xi = \sum_{q_z} A(q_z) B(q_z) |q_z| / \sum_{q_z} A^2(q_z) |q_z|$  is a parameter which is determined by the ratio of the spin-dependent and spin-independent parts of the electron-phonon interaction.

From Eqs. (7) it follows that, as expected, the contribution  $j_{\text{rel}}$  is independent of the polarization state of radiation and thus it may appear also for unpolarized radiation. Thus, for high temperatures, the temperature dependence of  $j_{\text{rel}}$  is described by the simple expression  $j_{\text{rel}} \propto n_s/k_B T$  because  $\eta \propto n_s$  and  $S_y \propto 1/k_B T$ . A fit of this function to the data is shown as

a solid line in Fig. 4(b) demonstrating good agreement. Treatment of the low temperature range needs allowance for terms of higher order in the in-plane phonon wave vector in the matrix element of electron-phonon interaction and is out of scope of this paper.

In addition to the magnetic field, polarization and temperature dependencies of the magnetophotocurrent we investigate its anisotropic properties. For that we vary the orientation of the in-plane magnetic field relative to the crystallographic direction. We observe that the magnitude of the current remains unchanged within the experimental accuracy for both  $\mathbf{j} \perp \mathbf{B}$  and  $\mathbf{j} \parallel \mathbf{B}$  geometries. This isotropic behavior of the current agrees well with the microscopic picture described above and it can be attributed to the fact that, in contrast to zinc-blende structure based QWs, structure inver-

sion asymmetry is the only possible asymmetry in conventional SiGe QWs.

Summarizing all data, we demonstrate that in asymmetric SiGe QWs spin-dependent scattering results in a pure spin current and spin separation. We show that application of an external magnetic field gives experimental access to investigations of pure spin currents. The basis of the method is the conversion of a pure spin current into an electric current by means of a magnetic field induced equilibrium spin polarization.

This work was supported by the DFG via Project GA 501/6-2 and Collaborative Research Center SFB689, the RFBR, programs of the RAS, the HBS, Russian Science Support Foundation, and in Austria by the "Fonds zur Förderung der Wissenschaftlichen Forschung," Vienna.

- <sup>1</sup>I. Zutíć, J. Fabian, and S. Das Sarma, *Rev. Mod. Phys.* **76**, 323 (2004).
- <sup>2</sup>Yu. A. Bychkov and E. I. Rashba, *Pis'ma Zh. Eksp. Teor. Fiz.* **39**, 66 (1984) [*JETP Lett.* **39**, 78 (1984)].
- <sup>3</sup>Z. Wilamowski, W. Jantsch, H. Malissa, and U. Rössler, *Phys. Rev. B* **66**, 195315 (2002).
- <sup>4</sup>A. M. Tyryshkin, S. A. Lyon, W. Jantsch, and F. Schäffler, *Phys. Rev. Lett.* **94**, 126802 (2005).
- <sup>5</sup>S. D. Ganichev, U. Rössler, W. Prettl, E. L. Ivchenko, V. V. Bel'kov, R. Neumann, K. Brunner, and G. Abstreiter, *Phys. Rev. B* **66**, 075328 (2002).
- <sup>6</sup>V. V. Bel'kov, S. D. Ganichev, P. Schneider, D. Schowalter, U. Rössler, W. Prettl, E. L. Ivchenko, R. Neumann, K. Brunner, and G. Abstreiter, *J. Supercond.* **16**, 415 (2003).
- <sup>7</sup>C. Tahan, M. Friesen, and R. Joynt, *Phys. Rev. B* **66**, 035314 (2002).
- <sup>8</sup>M. Fanciulli, P. Höfer, and A. Ponti, *Physica B* **340-342**, 895 (2003).
- <sup>9</sup>Z. Wilamowski and W. Jantsch, *Phys. Rev. B* **69**, 035328 (2004).
- <sup>10</sup>M. M. Glazov, *Phys. Rev. B* **70**, 195314 (2004).
- <sup>11</sup>C. Tahan and R. Joynt, *Phys. Rev. B* **71**, 075315 (2005).
- <sup>12</sup>E. Ya. Sherman, *Appl. Phys. Lett.* **82**, 209 (2003).
- <sup>13</sup>W. Jantsch, Z. Wilamowski, N. Sandersfeld, M. Mühlberger, and F. Schäffler, *Physica E (Amsterdam)* **13**, 504 (2002).
- <sup>14</sup>F. A. Baron, A. A. Kiselev, H. D. Robinson, K. W. Kim, K. L. Wang, and E. Yablonovitch, *Phys. Rev. B* **68**, 195306 (2003).
- <sup>15</sup>H. Malissa, W. Jantsch, M. Mühlberger, F. Schäffler, Z. Wilamowski, M. Draxler, and P. Bauer, *Appl. Phys. Lett.* **85**, 1739 (2004).
- <sup>16</sup>J. L. Truitt, K. A. Slinker, K. L. M. Lewis, D. E. Savage, C. Tahan, L. J. Klein, R. Joynt, M. G. Lagally, D. W. van der Weide, S. N. Coppersmith, M. A. Eriksson, A. M. Tyryshkin, J. O. Chu, and P. M. Mooney, *arXiv:cond-mat/0411735* (unpublished).
- <sup>17</sup>Z. Wilamowski, H. Malissa, F. Schäffler, and W. Jantsch, *arXiv:cond-mat/0610046* (unpublished).
- <sup>18</sup>S. D. Ganichev, E. L. Ivchenko, S. N. Danilov, J. Eröms, W. Wegscheider, D. Weiss, and W. Prettl, *Phys. Rev. Lett.* **86**, 4358 (2001).
- <sup>19</sup>S. D. Ganichev, E. L. Ivchenko, V. V. Bel'kov, S. A. Tarasenko, M. Sollinger, D. Weiss, W. Wegscheider, and W. Prettl, *Nature (London)* **417**, 153 (2002).
- <sup>20</sup>S. D. Ganichev and W. Prettl, *J. Phys.: Condens. Matter* **15**, R935 (2003).
- <sup>21</sup>V. V. Bel'kov, S. D. Ganichev, Petra Schneider, C. Back, M. Oestreich, J. Rudolph, D. Hägele, L. E. Golub, W. Wegscheider, and W. Prettl, *Solid State Commun.* **128**, 283 (2003).
- <sup>22</sup>E. L. Ivchenko, *Optical Spectroscopy of Semiconductor Nanostructures* (Alpha Science, Harrow, 2005).
- <sup>23</sup>M. Bieler, N. Laman, H. M. van Driel, and A. L. Smirl, *Appl. Phys. Lett.* **86**, 061102 (2005).
- <sup>24</sup>S. D. Ganichev and W. Prettl, *Intense Terahertz Excitation of Semiconductors* (Oxford University Press, Oxford, 2006).
- <sup>25</sup>C. L. Yang, H. T. He, Lu Ding, L. J. Cui, Y. P. Zeng, J. N. Wang, and W. K. Ge, *Phys. Rev. Lett.* **96**, 186605 (2006).
- <sup>26</sup>J. Hübner, W. W. Rühle, M. Klude, D. Hommel, R. D. R. Bhat, J. E. Sipe, and H. M. van Driel, *Phys. Rev. Lett.* **90**, 216601 (2003).
- <sup>27</sup>M. J. Stevens, A. L. Smirl, R. D. R. Bhat, A. Najmaie, J. E. Sipe, and H. M. van Driel, *Phys. Rev. Lett.* **90**, 136603 (2003).
- <sup>28</sup>H. Zhao, X. Pan, A. L. Smirl, R. D. R. Bhat, A. Najmaie, J. E. Sipe, and H. M. van Driel, *Phys. Rev. B* **72**, 201302(R) (2005).
- <sup>29</sup>S. A. Tarasenko and E. L. Ivchenko, *Pis'ma Zh. Eksp. Teor. Fiz.* **81**, 292 (2005) [*JETP Lett.* **81**, 231 (2005)].
- <sup>30</sup>Y. Kato, R. C. Myers, A. C. Gossard, and D. Awschalom, *Science* **306**, 1910 (2004).
- <sup>31</sup>J. Wunderlich, B. Kaestner, J. Sinova, and T. Jungwirth, *Phys. Rev. Lett.* **94**, 047204 (2005).
- <sup>32</sup>S. D. Ganichev, V. V. Bel'kov, S. A. Tarasenko, S. N. Danilov, S. Giglberger, Ch. Hoffmann, E. L. Ivchenko, D. Weiss, W. Wegscheider, Ch. Gerl, D. Schuh, J. Stahl, J. De Boeck, G. Borghs, and W. Prettl, *Nat. Phys.* **2**, 609 (2006).
- <sup>33</sup>E. L. Ivchenko and G. E. Pikus, *Izv. Akad. Nauk SSSR, Ser. Fiz.* **47**, 2369 (1983) [*Bull. Acad. Sci. USSR, Phys. Ser. (Engl. Transl.)* **47**, 81 (1983)].
- <sup>34</sup>S. A. Tarasenko, *Phys. Rev. B* **73**, 115317 (2006).
- <sup>35</sup>M. I. D'yakonov and V. I. Perel', *Zh. Eksp. Teor. Fiz. Pis'ma Red.* **13**, 657 (1971) [*JETP Lett.* **13**, 467 (1971)].

- <sup>36</sup>J. E. Hirsch, Phys. Rev. Lett. **83**, 1834 (1999).
- <sup>37</sup>S. A. Tarasenko, Pis'ma Zh. Eksp. Teor. Fiz. **84**, 233 (2006) [JETP Lett. **84**, 199 (2006)].
- <sup>38</sup>We consider here only the spin-dependent contribution induced by heteropotential asymmetry. Other terms are negligible in SiGe structures.
- <sup>39</sup>This is valid (i) for both the relaxation [Fig. 1(a)] and the excitation [Fig. 1(b)] mechanisms in the case of a nondegenerate distribution of carriers and (ii) for the excitation mechanism in the case of a degenerate distribution with the Fermi energy  $\varepsilon_F$  provided  $\hbar\omega < \varepsilon_F$  or  $\hbar\omega \gg \varepsilon_F$ .
- <sup>40</sup>Strictly speaking, the pure spin current, i.e., the flux of electron spins, is described by a second-rank pseudotensor with the components  $J_\beta^\alpha$  giving the flow in the  $\beta$  direction of spins oriented along  $\alpha$ , with  $\alpha$  and  $\beta$  being the Cartesian coordinates. Then, the electric current induced by imbalance of the pure spin photocurrent in magnetic field is given by  $j_\beta = 4e \sum_\alpha S_\alpha J_\beta^\alpha$ .
- <sup>41</sup>V. V. Bel'kov, S. D. Ganichev, E. L. Ivchenko, S. A. Tarasenko, W. Weber, S. Giglberger, M. Olteanu, H.-P. Tranitz, S. N. Danilov, Petra Schneider, W. Wegscheider, D. Weiss, and W. Prettl, J. Phys.: Condens. Matter **17**, 3405 (2005).
- <sup>42</sup>K. Seeger, *Semiconductor Physics* (Springer, Wien, 1997).